SOME ASPECTS OF THE DESIGN OF FIXED BED REACTORS FOR HYDROCARBON OXIDATION*

By

G. F. FROMENT

Rijksuniversiteit Gent, Belgium

(Received February 5, 1970)

I — The one-dimensional model with plug flow

The equations describing non-isothermal, non-adiabatic steady state operation are well known — for a single reaction $A \rightarrow B$ they may be written:

$$\frac{dx}{dz'} = \frac{\varrho_b M_m}{N_{A_0} G} r_A$$

$$\frac{dt}{dz'} = \varrho_b \frac{(-\Delta H)}{G c_p} r_A - \frac{4U}{G c_p d_t} t$$

The integration of this system of ordinary differential equations is generally non feasible by analytical methods. Numerical integration on digital computers presents no special difficulty. Besides, the analog computer is eminently suited for integration of such systems.

One particularly important aspect of the design of such reactors, especially encountered with exothermic reactions, is the so-called "stability" or better "parametric sensitivity". Indeed, with exothermic reactions the tubular reactor generally presents a "hot spot", a temperature peak. The problem is to choose the steady state inlet values of the parameters in such a way that the hot spot does not become excessive, even when these inlet values are subject to perturbations.

This sensitivity problem was first tackled by BILOUS & AMUNDSON [1] in an analytical way. They considered the transient continuity and energy equations for the reactor, linearized them around the steady state values in each point and studied the effect of a sinusoidal input perturbation. Predictions on the sensitivity are possible, provided one steady state profile has been calculated. This annihilates much of the benefit of the approach: once the computer program has been written in order to calculate one steady state profile

---

* Lecture held at the Department of Chemical Technology, Technical University of Budapest, October 3, 1969.

it is much easier to investigate the sensitivity by running the program a number of times for a set of values of the inlet parameters.

This is what **Barkelew** has done for the single reaction $A \rightarrow B$, with the aim of establishing a criterion for the parametric sensitivity [2]. The results are shown in Fig. 1.

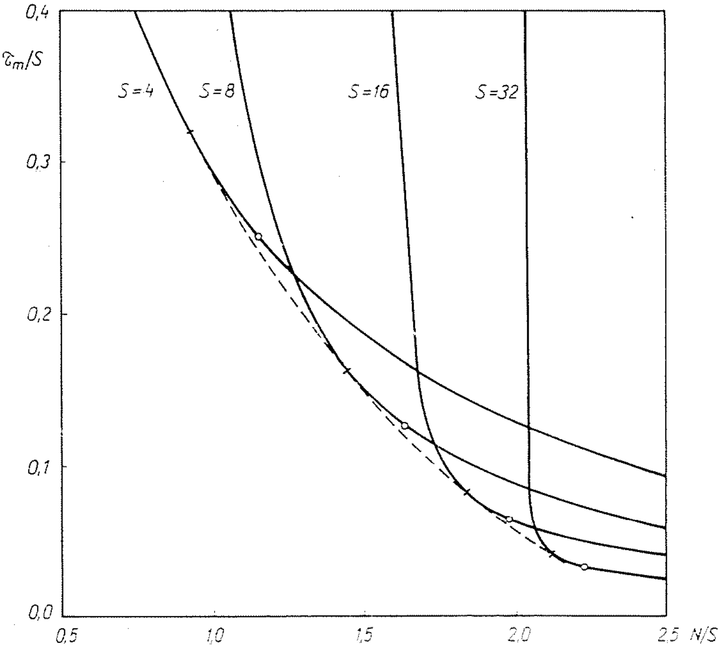

Fig. 1. Barkelew-diagram

N/S is the ratio of the rate of heat transfer per unit volume at $\tau = 1$, where $\tau = \frac{E}{RT_S^2}(T - T_S)$ to the rate of heat generation per unit volume at $\tau = 0$ and zero conversion i.e. at the entrance. $\tau_{\max}/S$ is the ratio of the dimensionless maximum temperature to the adiabatic temperature rise above the coolant temperature. A set of curves is obtained, with S as parameter. It is seen how the curves have an envelope which occurs very near to the knee of any individual curve. Above the tangent to the envelope $\tau_{\max}$ changes rapidly with N/S, below not.

The criterion **Barkelew** derived empirically says the reactor is stable with respect to small fluctuations if its maximum temperature is below the value at the tangent to the envelope.

Recently **Van Welsenaere** & **Froment** [3] tackled the problem in a different way. From an inspection of the temperature and partial pressure profiles in a fixed bed reactor they concluded extreme parametric sensitivity and runaway have to be feared when the hot spot exceeds a certain value and when the temperature profile develops inflexion points before the maximum. They transposed the peak temperature and the inflexion points into the $p - T$ plane. The loci of the maximum temperatures, called the "maxima-curve" and the loci of the inflexion points before the hot spot are shown in Fig. 2 as p_m and $(p_i)_1$, respectively. $(p_i)_2$ represents the locus of the inflexion point beyond the hot spot which is of no further interest in this analysis.

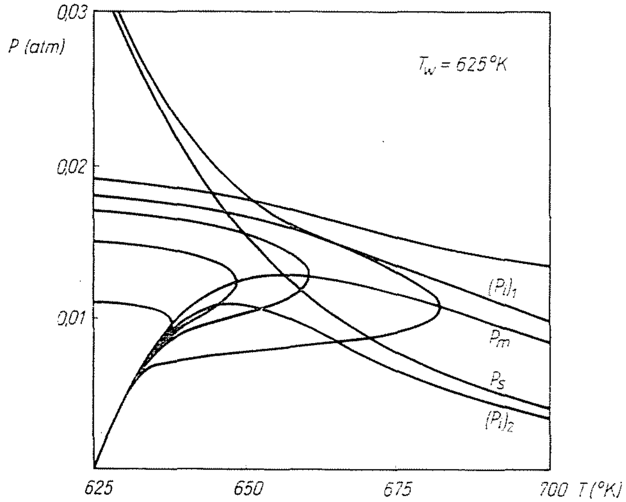

Fig. 2. $p - T$ phase plane, showing trajectories, maxima-curve, loci of inflexion points and "simplified" curve p_S

Two criteria were derived from this. The first states that runaway will occur when a trajectory — the $p - T$ relation in the reactor — intersects the maxima curve beyond its maximum. The second criterion states runaway will occur when a trajectory intersects the locus of inflexion points before the maximum. A more convenient version of this criterion is based on an approximation for this locus, represented by p_S in Fig. 2. Representation of the trajectories in the $p - T$ plane requires numerical integration but the critical points involved in the criteria are easily located. Two simple extrapolations from these points to the reactor inlet lead to upper and lower limits for inlet partial pressures and temperatures above which runaway will certainly occur and under which safe operation is guaranteed. Fig. 3 shows some results for a specific reaction. They are compared with those obtained from Barkelew's criterion, which is more complicated to use, though, $p^0_{l,1}$; $p^0_{u,1}$ and $p^0_{l,2}$; $p^0_{u,2}$ are upper and lower limits based upon the first and second criterion, resp.; $p^o_{m,1}$ and $p^o_{m,2}$ are their mean values; $p^\circ_{\mathrm{er},1}$ and $p^\circ_{\mathrm{er},2}$ are values obtained by numerical back integration from the critical points defined by the 1st and 2nd criterion onwards and in which the extrapolation is not involved.

The reaction considered here has pseudo first order kinetics and a heat effect suggested by gas-phase hydrocarbon oxidation. For a specific set of conditions the first criterion limits the hot spot to 31.6 °C, with $p_{l,1} = 1.35$ mole % and $p_{u,1} = 1.97$ mole %, the second criterion limits T to 29.6 °C while $p_{l,2} = 1.42$ and $p_{u,2} = 1.95$ mole %. By numerical integration of the system of differential equations what could be called "complete" runaway is obtained with $p_0 = 1.83$ mole %.

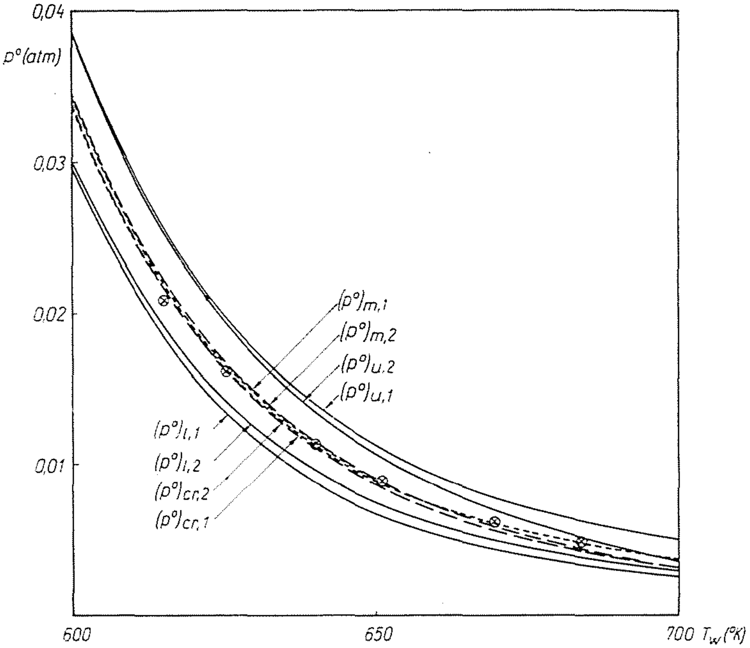

Fig. 3. Upper and lower limits, mean and exact critical value for the inlet partial pressure. Values derived from Barkelew's criterion are marked ⊗

The above criteria are therefore believed to be of great help in first stages of design since they permit a rapid and accurate selection of operating conditions, prior to any work on the computer. They are, however, limited to single reactions. Nothing like this is available for a complex reaction system, with its large number of parameters. Complex cases will probably always be handled individually.

In the preceeding the parametric sensitivity was investigated by considering the steady state only. LIU & AMUNDSON focused their attention more upon the stability, sensu stricto [32]. They were more concerned with the question if the profiles in an adiabatic reactor return to the original steady state or not after removal of a perturbation. Therefore they integrated the transient equations describing the state of both the fluid and solid numerically along the characteristics. The stability was shown to depend upon the state of the individual particles. Indeed, for a certain range of the variables more than one steady state is possible. With each particle having only one steady state unique temperature and conversion profiles are obtained. These profiles are stable: after removal of a perturbation the system returns to its original state. With particles having multiple steady states the concentration and temperature profiles are non-unique, and dependent upon the initial state of the bed. Large perturbations, after removal, may leave the reactor in an entirely different state. LIU, ARIS & AMUNDSON also considered the non-adiabatic reactor [32].

It has been proposed to refine the one-dimensional model by adding a term taking mixing in axial direction into account. This leads to a second order differential equation. The most complete investigation of this model was carried out by CARBERRY & WENDEL for the reaction $A \rightarrow B \rightarrow C$ [31]. Inter- and intraparticle heat and mass transfer was also considered. The effect of axial mixing was found to be negligible unless one is dealing with extremely shallow beds. The gradients within the particle are of great importance.

There are several objections which may be formulated against the one-dimensional model.

The first concerns the velocity profile, which is not flat, as was shown e.g. by SCHWARTZ & SMITH [4, 5]. The second — and most serious — concerns the radial temperature profile. Indeed, the temperature in a cross-section of the reactor can only be uniform when the resistance to radial heat transfer is zero. This condition is evidently not fulfilled, owing to the poor conductivity of catalyst supports, so that radial gradients are inevitable in non isothermal, non-adiabatic catalytic reactors. Whenever it is to be feared that important overtemperatures in the axis may have detrimental effects on the process selectivity or catalyst activity there is a need for design models which permit the prediction of the detailed temperature and conversion patterns in the reactor. Such design models are of two-dimensional nature. Depending upon the underlying concept they can be classified in two broad categories:

1. Those based upon the effective transport concept, in which all transport, except that by the overall flow, is treated as a diffusion — or conduction — like phenomenon. This is the approach used by BARON [34], SMITH [35], BEEK [36], MICKLEY & LETTS [37] and FROMENT [33].

2. Those based upon the mixing cell concept, in which all transport, except that by the overall flow, is considered as resulting from a sequence of mixing events taking place in a two-dimensional network of cells with complete mixing. Whereas the first approach leads to a boundary value problem, the second leads to an initial value problem. The mixing cell model was first applied to the two-dimensional case by DEANS & LAPIDUS, who mainly described the computational aspects [38]. It was further used by MCGUIRE & LAPIDUS

who studied in detail the stability of the two-dimensional case, to which they extended SHEAN-LIN LIU & AMUNDSON's work [39]. They focused their attention exclusively upon the rather special situation in which multiple steady states are possible for the particles. MCGUIRE & LAPIDUS distinguished between the gas and solid temperature and took gradients within the particles into account. As they had to deal with the transient equations the computational effort almost became prohibitive. AGNEW & POTTER extended the BARKELEW criterion for so-called stability to the two-dimensional model, using the mixing cell concept [44]. In what follows an effective transport model is set up and its application to a realistic case involving yield problems is discussed. Particular attention is given to the problem of parametric sensitivity. Simultaneously some insight will be gained into the reliability of the one-dimensional model described above. Before this can be done, however, it may be useful to review briefly some aspects of heat and mass transfer in packed beds.

II — The two-dimensional model for heat and mass transfer in packed beds

II.A. — Mass transfer in packed beds

The hydrodynamics of packed beds are so complex that it is practically impossible to describe them rigorously. Even if it were possible, the resulting equations would be so complex as to defy practical application. Faced with such a situation the chemical engineer uses mathematical models to simulate the real behaviour. The model generally used to day superposes upon the transfer by the overall flow an additional transfer, the formulation of which is based upon the observation that the travel of a fluid element between two points in a packed bed is built up of a large number of random steps, due to the random orientation of the passages between the packing.

The flux due to such a process may be described by a formula completely analogous to Fick's 1st law of diffusion. In the case of a packed bed the proportionality constant in this law is called the effective diffusivity. It is a function of both the flow conditions and the properties of the fluid. As packed beds are not isotropic for this effective diffusion, two components, one in axial and one in radial direction, have been considered.

When the fluxes due to effective diffusion are superposed upon the flux due to the overall flow the following continuity equation is obtained for a component flowing in the steady state through a cylindrical packed bed, in the absence of reaction

$$u(r')\frac{\partial c}{\partial z'} = \frac{\partial}{\partial z'}\left[D'_L(r')\frac{\partial c}{\partial z'}\right] + \frac{1}{r'}\frac{\partial}{\partial r'}\left[D'_R(r')\frac{\partial c}{\partial r'}\right]$$

an equation which is generally further simplified into

$$u \frac{\partial c}{\partial z'} = D_L \frac{\partial^2 c}{\partial z'^2} + \frac{D_R}{r'} \frac{\partial}{\partial r'} \left(r' \frac{\partial c}{\partial r'} \right)$$

where D_R is nothing but the mean of $D'_R(r')$, but where D_L differs from the mean of $D'_L(r')$ because of the effect of the velocity profile [43]. The major part of the data available in the literature pertain to the class D_R and D_L. We will not discuss the methods for obtaining D_R and D_L from residence time distribution data, but we will briefly review the results which are of interest to the design of chemical reactors.

II.A.1. — Radial effective diffusivity, D_R

The available data are brought together in a Pe_{mR} vs Re-diagram shown as Fig. 4.

Owing to wall effects, the importance of which grows with increasing d_p/d_t, it is found that Pe_{mR} also depends on d_p/d_t. The data of Dorrweiler & Fahien [8] and Fahien & Smith [6] obtained at several d_p/d_t are correlated empirically by using as an ordinate $Pe_{mR} \left[1 + 19{,}4 \left(\frac{d_p}{d_t} \right) \right]$, rather than Pe_{mR} itself.

It is to be noted that Hiby's experiments, free of wall effects, lead to higher Pe_{mR} [10].

In the laminar flow range the contribution of molecular diffusion is significant and Pe_{mR} depends on the properties of the fluid, expressed by the Schmidt number. In the turbulent flow range, however, D_R has been found

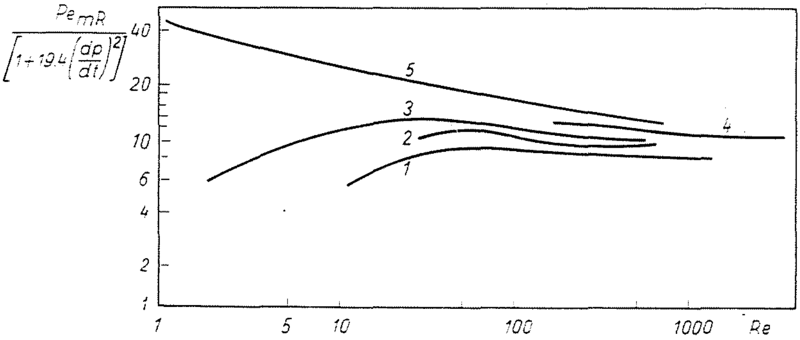

Fig. 4. Radial effective diffusivity data. 1. — Fahien & Smith [6]. 2. — Bernard & Wilhelm [7]. 3. — Dorrweiler & Fahien [8]. 4. — Plautz & Johnstone [9]. 5. — Hiby [10]

to vary proportionally with the flow velocity so that Pe_{mR} becomes independent of *Re*.

For practical applications we will note that Pe_{mR} is lying between 8 and 11.

II.A.2. — Axial effective diffusivity

The available data are shown in Fig. 5, again in a *Pe* vs *Re*-diagram. The data obtained by McHenry & Wilhelm for gases indicate that Pe_{mL} too is independent of *Re* in the higher flow range [11]. The data for liquids slowly tend towards those for gases. Hiby has measured D_L values in absence of wall effects with liquids [10]. The values are considerably higher and close to those for gases. This would indicate that the D_L values strongly depend on the velocity profile and short-circuiting effects.

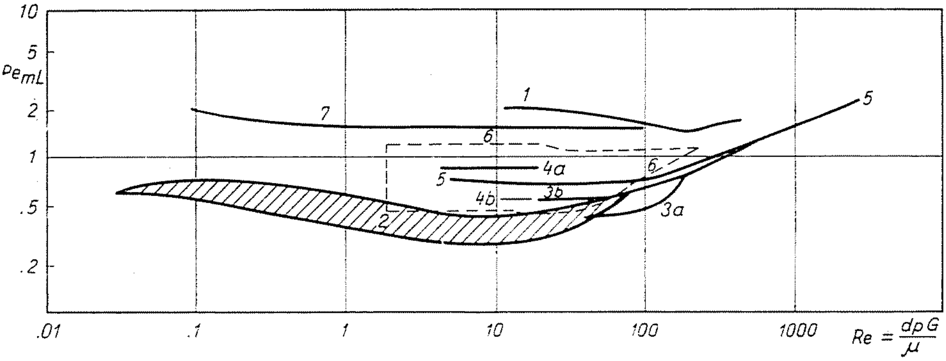

Fig. 5. Axial effective diffusivity data. 1. — Mc Henry & Wilhelm [11]. 2. — Ebach & White [12]. 3a. — Carberry & Bretton [13]. b. — idem. 4a. — Strang & Geankoplis [14]. b. — idem. 5. — Cairns & Prausnitz [15]. 6. — Hiby [10]. 7. — Hiby — without wall effect [10]

For design purposes Pe_{mL} may be considered to lie between 1 and 2.

II.B. — Heat transfer in packed beds

The transfer of heat in packed beds is even more complicated, because the solid phase participates in it and radiation also has to be taken into account.

The transfer is split into 2 main categories: on one hand convection by plug flow, on the other hand all the other effects. In order to describe the latter without complicating the design equations prohibitively, the bed consisting of fluid and solid is considered as a homogeneous body, through which heat is transferred by effective conduction. This effective conduction is superposed upon the overall convection, supposed to be of the plug flow type. A heat balance on a differential element in the steady state and in the absence of reaction then takes a form completely analogous to that of the continuity equation:

$$\lambda_R \left[\frac{\partial^2 t}{\partial r'^2} + \frac{1}{r'} \frac{\partial t}{\partial r'} \right] + \lambda_L \frac{\partial^2 t}{\partial z'^2} - G c_p \frac{\partial_t}{\partial z'} = 0$$

when the bed is considered to be anisotropic for "effective" conduction and λ_R, λ_L and G are independent of the radial position. Yet, upon measuring λ_R experimentally it is observed that it decreases considerably in the vicinity of the wall, probably because of variations in packing density — it is as if a supplementary resistance is experienced near the wall. Two attitudes may be taken: either use a mean λ_R or consider λ_R as being constant at the value n the central core and introduce a wall heat transfer coefficient α_w, defined by:

$$\alpha_w(t_R - t_w) = - \lambda_R \left(\frac{\partial_t}{\partial r'} \right)_w$$

Generally the second approach is preferred.

II.B.1. — Radical effective thermal conductivity

Fig. 6 shows the most reliable data obtained until now for λ_R. It is seen how λ_R varies linearly with *Re*. The line representing KWONG & SMITH's data gives an idea of the influence of the conductivity of the solid itself, in this case steel [19].

Strictly speaking these results are restricted to the conditions under which they were obtained. They do not provide any means for extrapolation to other conditions — this requires a model for heat transfer in packed beds.

The most elaborate model available to day is due to YAGI & KUNII [21] and KUNII & SMITH [20], but it goes back to pioneering work by SINGER & WILHELM [22]. The model considers the heat flux by effective conduction as resulting from 2 contributions, one static, the other dynamic. The static contribution, measured in the absence of flow, considers heat transferred in the fluid and the solid by conduction and radiation.

The dynamic contribution may be predicted on the basis of data on effective radial diffusivity. The straight line numbered 5 in Fig. 6 is calculated on the basis of this theoretical model for the mean conditions of the reported experiments. The agreement is quite satisfactory.

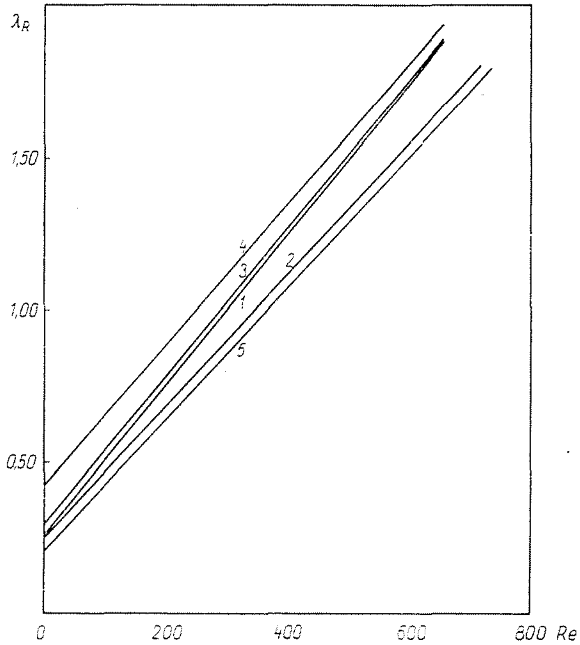

Fig. 6. Effective thermal conductivity data. 1. — Coberly & Marshall [16]. 2. — Campbell & Huntington [17]. 3. — Calderbank & Pogorsky [18]. 4. — Kwong & Smith [19]. 5. — Kunii & Smith [20]

II.B.2. — Wall heat transfer coefficient

The available data are reviewed in Fig. 7 which shows considerable spread.

Early correlations of the form $\frac{\alpha_w d_p}{\lambda_g} = mRe^n$ are only valid from a certain Re upwards, as they would predict a zero value for α_w at $Re = 0$, which is not correct. Therefore, Yagi & Kunii proposed an equation of the type

$$\frac{\alpha_w d_p}{\lambda_g} = \frac{\alpha_w^o d_p}{\lambda_g} + \psi \, Pr \, Re$$

where α_w^0 may be calculated on the basis of a model analogous to the one proposed for the static contribution to λ_R [26]. It should be pointed out here that α_w is fundamentally different from the so-called "overall" heat transfer coefficients measured by Colburn [30], Leva [27], Maeda [29] and Verschoor & Schuit [28] e.g. which are based on mean temperatures in the bed, as if there were no radial gradients, in other words, as if there were no resistance to heat transfer in the central core.

We will not enter into details about λ_L, the effective thermal conductivity in axial direction. In industrial reactors the flux due to axial effective conduction may be neglected compared to that due to the overall flow [31].

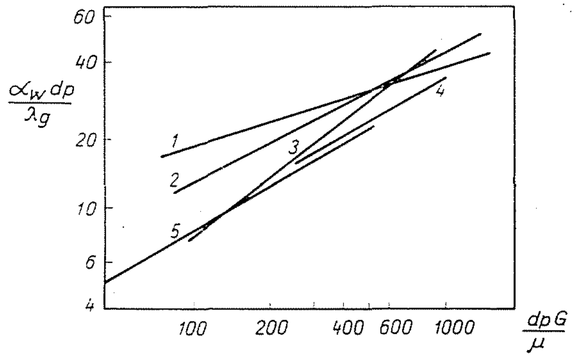

Fig. 7. Wall heat transfer data. 1. — Coberly & Marshall [16]. 2. — Hanratty (cylinders) [23]. 3. — Hanratty (spheres) [23]. 4. — Yagi & Wakao [24]. 5. — Yagi, Kunii & Wakao [25]

III — Design of fixed bed catalytic reactors based on effective transport models

So far a two-dimensional model for predicting temperature and concentration gradients in packed beds was established and the experimental data, required for its application, were reviewed. The treatment can easily be extended to the fixed bed catalytic reactor by completing the continuity and energy equations with terms accounting for the reaction. This leads to a system of non-linear second order partial differential equations, the integration of which is non feasible by analytical methods.

There exists a graphical procedure for integration of the system with the true rate equation proposed by Schmidt and applied by Baron [33] but it is not sufficiently precise and very tedious. Even for the digital computer the numerical integration of a system of non-linear, second-order, partial differential equations is a serious problem, for reasons of mathematical stability of the solution. Beek discussed this integration and carried it out for a reaction $A \rightarrow B$ and a set of typical values of the parameters [36]. Mickley & Letts [37] used an implicit difference formulation but with explicit evaluation of nonlinear terms. They applied it to the reaction $A \rightarrow B \rightarrow C$ and calculated the influence of radial gradients on the yield.

In Gent the implicit Crank-Nicolson procedure has been adopted [33]. The details of it have been discussed [41]. The program was tried out in 1961 and has been applied since to several cases.

The case considered here is of a rather complex nature, namely

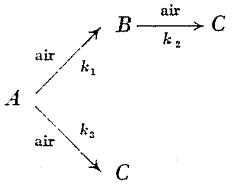

This reaction model is fairly representative of the gas phase air oxidation of o-xylene into phthalic anhydride on V_2O_5 catalysts. A represents o-xylene, B phthalic anhydride and C the final oxidation products CO and CO_2.

Air is used in very large excess: the o-xylene mole fraction is generally kept below 1%, so as to stay under the explosion limit. One way of carrying out this very exothermic process is to use a multitubular reactor, consisting e.g. of 2500 tubes of 2.5 cm diameter, 2.5 to 3 m long, packed with catalyst and cooled by a salt bath that transfers the heat of reaction to a steam generator. Owing to the very large excess of oxygen the rate equations may be considered in first approximation to be of the pseudo 1st order type; so that at atmospheric pressure:

$$r_T = (k_1 + k_3)\, N_{A_0} \cdot N_0\, (1 - y)$$

$$r_B = N_{A_0} \cdot N_0 \cdot [k_1(1 - y) - k_2 x]$$

$$r_C = N_{A_0} \cdot N_0 \cdot [k_2 x + k_3\, (1 - y)]$$

with $y = x + w$

$$\ln k_1 = -\frac{27{,}000}{1{,}98\,(t + T_0)} + 19{,}837$$

$$\ln k_2 = -\frac{31{,}400}{1{,}98\,(t + T_0)} + 20{,}86$$

$$\ln k_3 = -\frac{28{,}600}{1{,}98\,(t + T_0)} + 18{,}97$$

When use is made of the following dimensionless variables

$$z = \frac{z'}{d_p} \qquad r = \frac{r'}{d_p} \qquad t = T - T_0 \qquad R = \frac{R'}{d_p}$$

the steady state continuity and energy equations may be written in cylindrical coordinates

$$\left\{\begin{aligned} \frac{\partial x}{\partial z} &= a_1\left(\frac{\partial^2 x}{\partial r^2}+\frac{1}{r}\,\frac{\partial x}{\partial r}\right)+b_1 r_B \\ \frac{\partial_w}{\partial z} &= a_1\left(\frac{\partial^2 w}{\partial r^2}+\frac{1}{r}\,\frac{\partial w}{\partial r}\right)+b_1 r_C \\ \frac{\partial t}{\partial z} &= a_2\left(\frac{\partial^2 t}{\partial r^2}+\frac{1}{r}\,\frac{\partial t}{\partial r}\right)+b_2 r_B+b_3 r_C \end{aligned}\right. \tag{1}$$

Note that the term for axial effective transport was dropped in these equations. At the high flow rates used in practice the contribution of this mechanism may indeed be neglected.

The constants in these equations have the following meaning:

$$a_1=\frac{D_R\,\varrho_f}{G_i\,d_p}=\frac{1}{Pe_{mR}} \qquad b_1=\frac{\varrho_b\,d_p\,M_m}{G(N_A)_0}$$

$$a_2=\frac{\lambda_R}{G\,C_p\,d_p}=\frac{1}{Pe_{hR}} \qquad b_2=\frac{\varrho_b\,d_p\,(-\Delta H_1)}{G_0\,C_\mathrm{p}}$$

$$b_3=\frac{\varrho_b\,d_\mathrm{p}\,(-\Delta H_3)}{G\,C_p}$$

The boundary conditions are as follows:

$$x=0 \qquad w=0 \qquad \text{at} \quad z=0$$

$$\frac{\partial x}{\partial r}=0 \qquad \frac{\partial w}{\partial r}=0 \qquad r=0$$

$$r=R$$

$$t=0 \qquad z=0 \qquad 0\leq r\leq R$$

$$\frac{\partial t}{\partial r}=0 \qquad \mathrm{r}=0$$

$$\left(\frac{\partial t}{\partial r}\right)_R=-\frac{\alpha_w\,d_p}{\lambda_R}\,t=-\alpha\,t$$

In the last boundary condition the resistance of the tube wall itself and the outside wall resistance are neglected.

Bulk mean values are obtained by

$$\zeta_m = 2\int_0^1 \zeta \frac{r}{R} d\left(\frac{r}{R}\right)$$

The following typical data were used in the calculations:

$(N_A)_0 = 0.00924$ — which corresponds to 44 g/Nm^3; $(N_{0x})_0 = 0.208$; $\Delta H_1 = -307$ Kcal/gmole; a single value of $\Delta H_3 = -1.090$ Kcal/gmole for the formation of CO and CO$_2$; $d_t = 0.025$ m; $d_p = 0.003$ m; $\varrho_b = 1300$ kg/m^3; $G_0 = 4.684$ kg/m^2.hr. It follows that $Re = 121$. From Kunii & Smith's equation [20] $\lambda_R = 0.67$ Kcal/m.hr.°C, from Yagi & Wakao's equation [24] $\alpha_w = 134$ Kcal/m^2.hr.°C, so that $Pe_{hR} = 5.25$, whereas $Pe_{mR} = 10$. In all cases the feed inlet temperature equalled that of the salt bath.

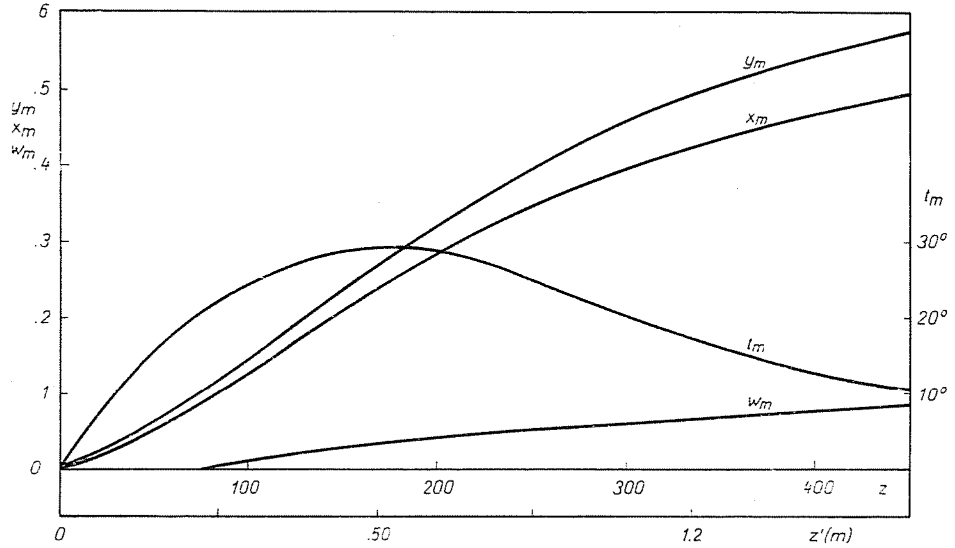

Fig. 8. Radial mean conversions and temperature as a function of bed length

Fig. 8 shows the result obtained for an inlet temperature of 357 °C. The bulk mean conversions and temperatures are plotted as a function of reactor length. The conversion to phthalic anhydride tends to a maximum, which is not shown on the figure and which is typical for consecutive reaction systems.

Typical also for exothermic systems is the "hot spot", where t_m equals about 30 °C. Even for this case, which is not particularly drastic, the radial temperature gradients are severe, as may be seen on Fig. 9. The temperature in the axis is well above the mean. So much for the inlet temperature of

357 °C, where a length of 3 m is insufficient to come to the maximum in phthalic anhydride concentration. What happens when the temperature is raised by only 3 °C to overcome this, is shown in Fig. 10.

It is seen how the temperature rise goes out of control — a nice example of "parametric sensitivity".

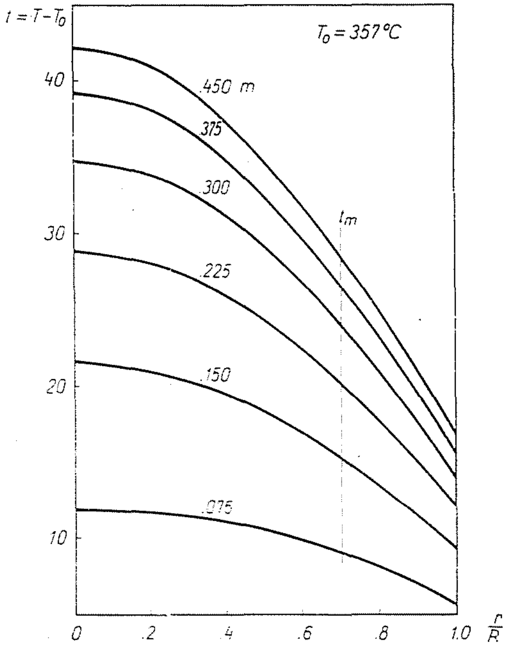

Fig. 9. Radial profiles of temperatures at several bed lengths

It should be remarked here that the upper part of curve 1 may be considerably in error, because heat transfer between gas and solid may become rate-controlling. To take this phenomenon into account would require the addition of equations to the system (1) — the effective transport concept does not distinguish between the gas and solid temperatures. There can be no doubt, however, about the existence of critical conditions for a feed temperature of 360 °C. The "hot spot" experienced under these conditions, even less dramatic than shown in Fig. 9, may be detrimental for the catalyst. Even if it were not, important "hot spots" would be unacceptable for reasons of selectivity. Indeed, the kinetic equations are such that the side reactions are favored by increasing the temperature. Just how detrimental the influence of the hot spot on the selectivity or yield is can be seen on Fig. 11, in which the yield is plotted as a function of total conversion for several inlet temperatures. A few percentages more in yield, due to judicious design and operation, are important in high tonnage productions.

The inlet temperature is not the only parameter determining the runaway temperature. The influence of the hydrocarbon inlet concentration is shown in Fig. 11 which summarizes Fig. 9 obtained with 44 g/Nm^3 and two more diagrams like Fig. 9, but obtained with 38 and 32 g/Nm^3. Fig. 12 shows how the runaway limit rises with decreasing hydrocarbon inlet concentration. The other curves given in the diagram show the inlet temperatures which lead to hot spots of 43 and 30 °C.

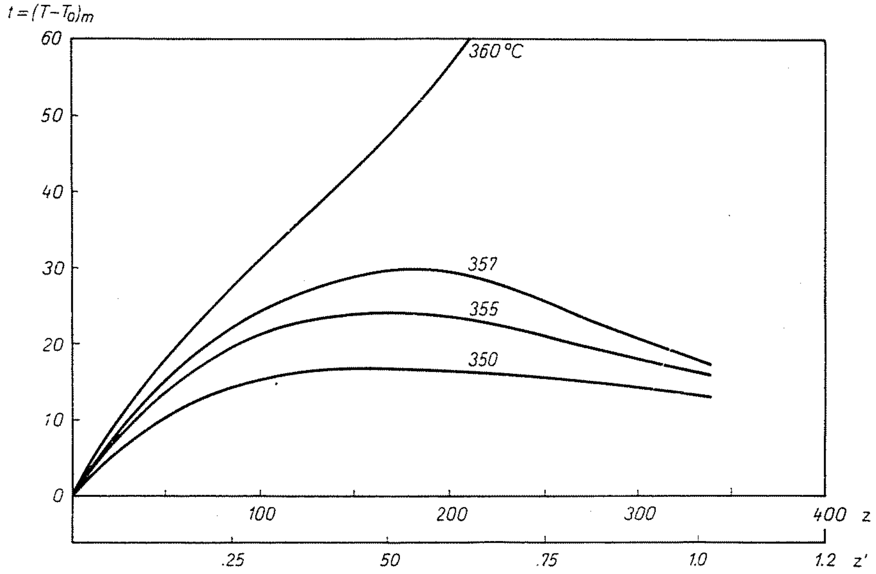

Fig. 10. Radial mean temperature as a function of bed length for several inlet temperatures

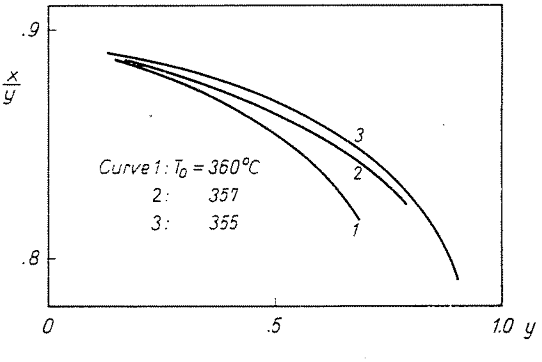

Fig. 11. Outlet selectivity as a function of total conversion for several inlet temperatures

It follows from the calculations leading to Figs 7 and 9 that with 44 g/Nm^3 an inlet temperature of 357 °C is insufficient to realize the desired

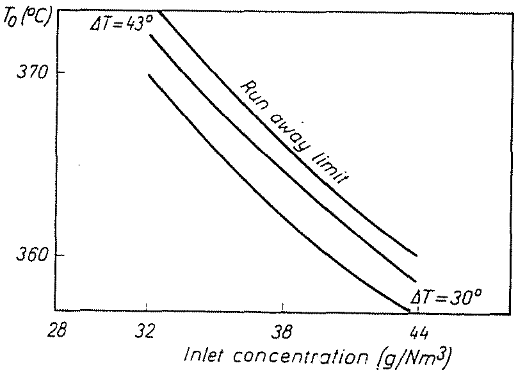

Fig. 12. Effect of inlet concentration on runaway limit

conversion in the given length of 2.5 to 3 m, while an inlet temperature of 360 °C causes runaway. Obviously, nobody would take the risk of running the reactor within such narrow temperature limits. If it is impossible to increase the bed length the calculations show that for the range of inlet concentrations considered the hot spot has to exceed 30 °C. Fig. 11 reveals operation within the region of extreme sensitivity is inevitable. No gain in safety margin is to be expected from a decrease in inlet concentration. Moreover, such a measure would decrease the production capacity and influence un-

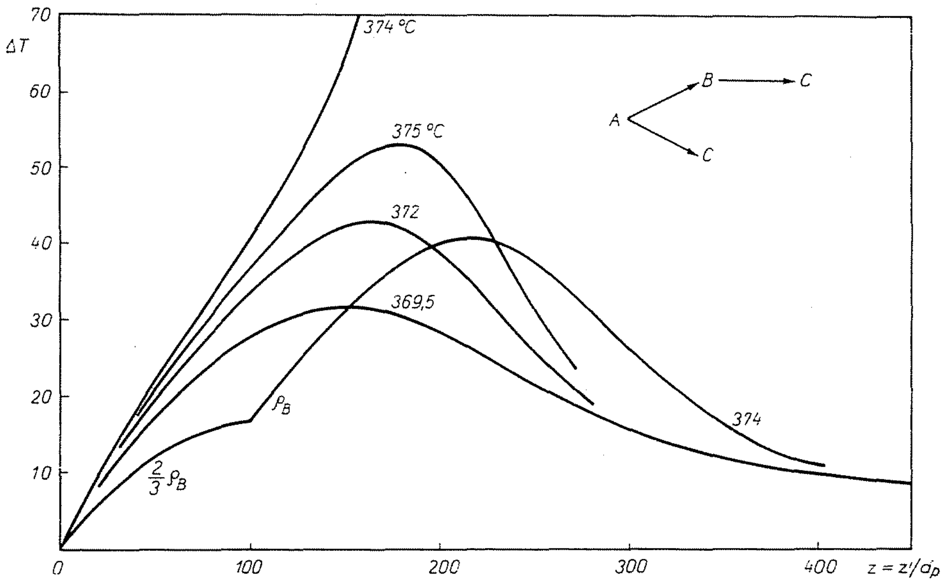

Fig. 13. Effect of diluting the catalyst by means of inert packing material. Two-dimensional model

favorably the economics of the plant. With the given length there seems to be only one way out, that is to realize an entirely different type of temperature profile, showing no real hot spot, but leading altogether to a higher average temperature. An appropriate dilution of the catalyst with inert packing in the early sections of the bed would make this possible.

This can be realized in practice by suitable dilution of the catalyst with inert material, as is illustrated in Fig. 13. The curves of this figure were calculated for an inlet concentration of 32 g/Nm^3, which leads to runaway with an inlet and wall temperature of 374 °C. Replacing one third of the catalyst by inert material in the entrance zone allows operation under these conditions without risking runaway.

IV — Comparison of the results based on the one- and two-dimensional models

For the one-dimensional model with plug flow the system of equations (1) reduces to:

$$\left\{\begin{aligned} \frac{dx}{dz} &= b_1 r_B \\ \frac{dw}{dz} &= b_1 r_C \\ \frac{dt}{dz} &= -\frac{4U}{G c_p d_t} t + b_2 r_B + b_3 r_C \end{aligned}\right.$$

The coefficient U is an "overall" heat transfer coefficient obtained under the assumption that the resistance to heat transfer is localized in a thin film near the wall [27, 29, 30].

If the predictions based on the one-dimensional model are to be compared with those based on the two-dimensional model it is necessary to use the same heat transfer data in both models. In other words it is necessary to build up U from λ_R and α_w.

This can be done in the following way [32, 45].

The temperature in a packed bed heat exchanger in which there is no reaction may be written, when the gradients are not accounted for:

$$\bar{t}' = e^{-Kz} \qquad \text{where} \qquad t' = \frac{T - T_0}{T_0 - T_s}$$

$$K = \frac{4U}{G c_p d_t}$$

but when the gradients are accounted for:

$$t'(r,z) = 2\alpha R \sum_{n=0}^{\infty} \frac{e^{-\frac{a^2}{R^2}\lambda_n^2 z} J_0\left(\lambda_n \frac{r}{R}\right)}{(\lambda_n^2 + \alpha^2 R^2)\, J_0(\lambda_n)}.$$

λ_n are the positive roots of $\dfrac{1}{\alpha R} = \dfrac{J_0(\lambda_n)}{\lambda_n J_1(\lambda_n)}$ and $\alpha = \dfrac{Ud_p}{\lambda_e}$

$$t'_m = 2 \int_0^1 t \frac{r}{R}\, d\left(\frac{r}{R}\right)$$

$$t'_m = 4\alpha^2 R^2 \sum_{n=0}^{\infty} \frac{e^{-\frac{a_2}{R^2}\lambda_n^2 z}}{\lambda_n^2(\lambda_n^2 + \alpha^2 R^2)}$$

If $\bar{t}'$ is to match as close as possible t'_m, the parameter K has to be such that the exponential function $\bar{t}'(z)$ matches a sum of exponential functions. The value of K achieving this in the best possible way may be obtained from the condition that the moments of zero order of both equations be equal. This fleads to:

$$\frac{1}{K} = \frac{4\alpha^2 R^2}{a^2} \sum_{n=0}^{\infty} \frac{1}{\lambda_n^4(\lambda_n^2 + \alpha^2 R^2)}$$

rom which [32]:

$$K = \frac{2a_2}{R} \cdot \frac{4\alpha}{R+4}$$

or finally

$$\frac{1}{U} = \frac{1}{\alpha_w} + \frac{R'}{4\lambda_R}$$

Using the λ_R and α_w correlations of KUNII & SMITH [20] and YAGI & WAKAO [24] used in the two-dimensional calculations it becomes possible to calculate U. It is found to be 82.7 Kcal/m^2.hr.°C. This value is used in the one-dimensional calculations shown in Fig. 14, which is to be compared with Fig. 10. The two-dimensional model predicts a runaway of the reactor for an inlet temperature of 360 °C.

The one-dimensional model predicts a temperature rise of only 40 °C at an inlet temperature of 362°, a rise of 48° at an inlet temperature of 363°. The runaway temperature is now found to be 365 °C. The discrepancy between the predictions of the one- and two-dimensional models grows as the hot spot increases in magnitude. Some conclusions seem justified at this point.

By its very essence the one-dimensional model cannot provide any information about the detailed temperature and conversion pattern in the reactor. It was shown that, except for "mild" conditions, it may also fail to predict the mean temperatures and that the predicted values are always low for exothermic reactions.

Yet, for practical purposes, the prediction of the runaway limit within a five degrees agreement with the two-dimensional model has to be considered as excellent. Being much more tractable, the one-dimensional model will continue to be used for exploratory purposes and transient studies. The final calculations may be carried out on the basis of the two-dimensional model, particularly where considerable overtemperatures in the axis are to be feared for reasons of catalyst stability, process selectivity or simply safe operation. To date the computer possibilities are such that the use of the two-dimensional model presents no difficulties when applied to the steady state.

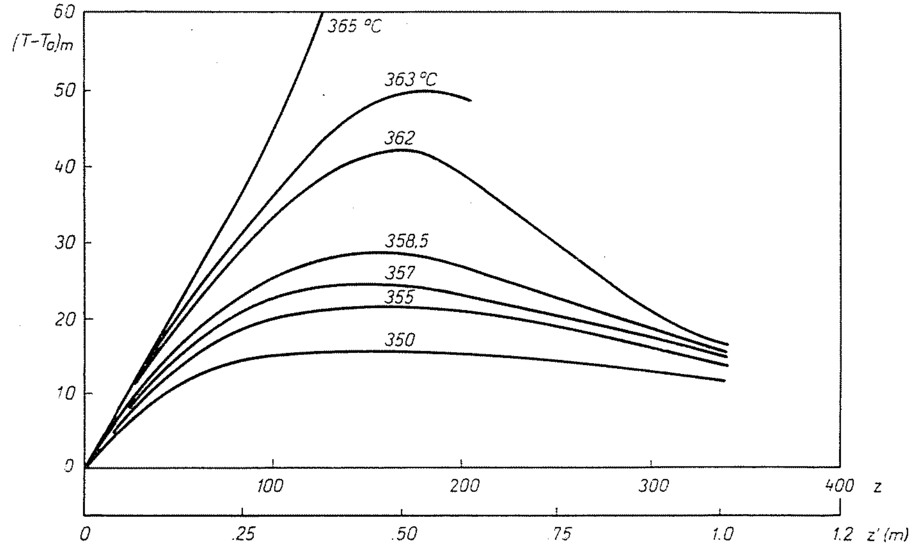

Fig. 14. One-dimensional model. Temperature profiles for various inlet temperatures

There remains the question how reliable our calculations, even those based on the most elaborate model, can be today. Their reliability depends, of course, on the value of the model itself and on the experimental parameters used in it. The next paragraph throws some light on the latter point.

V — Influence of some of the parameters of the models

The calculations for the two-dimensional model were repeated for several situations, drastic or not, but with $Pe_{mR} = 8$ instead of 10. The influence on the temperature and conversion profiles was completely negligible. It would therefore seem our mixing data need not be refined any further, at least for the usual situations. In order to get a feeling for the importance of the heat transfer parameters, calculations were performed with values of α_w and λ_e about 10% higher than those used in the calculations reported in Fig. 10.

Fig. 15 shows the temperature profile obtained for an inlet temperature of 360 °C, but with $\lambda_e = 0.75$ Kcal/m.hr.°C, instead of 0.67 and with an unchanged value for α_w of 134 Kcal/m^2.hr.°C.

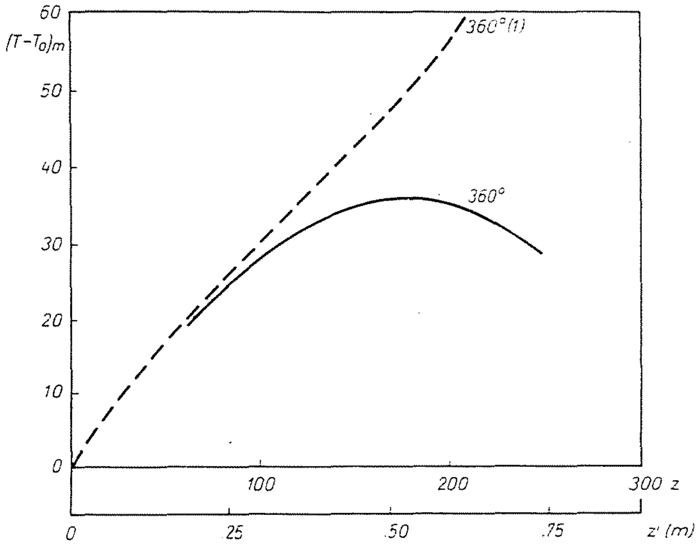

Fig. 15. Influence of varying the effective thermal conductivity on the radial mean temperature profile

The resulting overall coefficient U amounts to 86 Kcal/m^2.hr.°C, instead of 82.7 for the reference curve "360" of Fig. 9. The maximum mean over-temperature is now reduced to about 35 °C.

Fig. 16 shows the temperature profile obtained for the inlet temperature of 360° again, but with $\alpha_w = 150$ Kcal/m^2.hr.°C instead of 134 and an unchanged λ_R of 0.67 Kcal/m^2.hr.°C. The corresponding overall coefficient is 88 Kcal/m^2.hr.°C. Again the radial mean temperature rise is reduced to about 35 °C. Fig. 14 also compared the curves obtained for a feed temperature of 357 °C. The influence of α_w is less pronounced, of course, for this milder situation.

Variations in the values of the heat transfer coefficients of the order of 10% are well within the spread of the experimental results. This is illustrated by Figs 15—16, and for U by Fig. 17, which compares overall coefficients built up from λ_R and α_w data of Kunii & Smith [20] and Yagi & Wakao [24] with these obtained by Leva [27], Maeda [29] and Verschoor & Schuit [28]

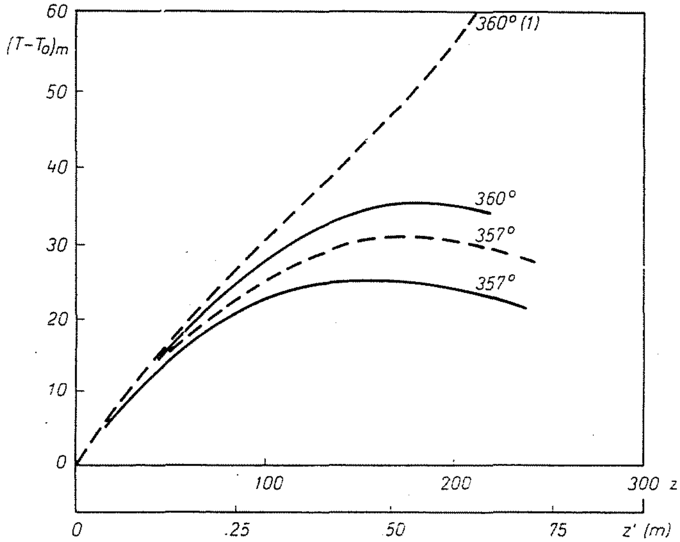

Fig. 16. Influence of varying the wall heat transfer coefficient on the radial mean temperature profile

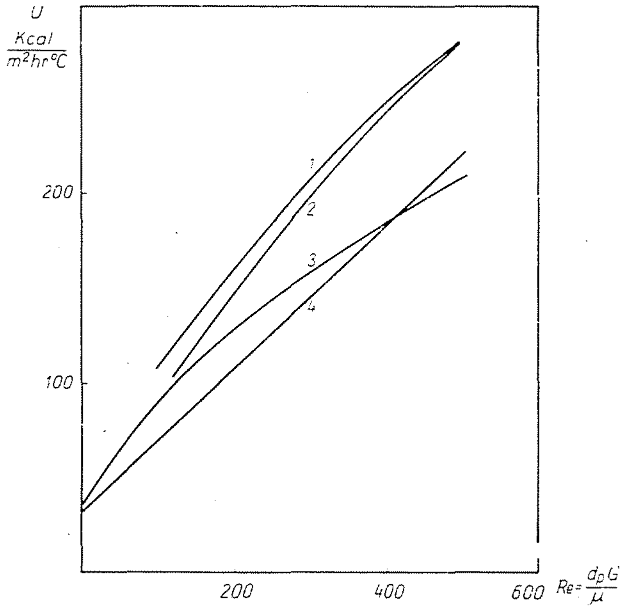

Fig. 17. Comparison of overall heat transfer coefficient-data. 1. — Maeda [29]. 2. — Leva [27]. 3. — Verschoor & Schuit [28]. 4. — Yagi & Kunii [21, 26]

This figure clearly illustrates our continuing need for further research on heat transfer in packed beds.

Recently De Wasch & Froment determined λ_{er}, and α_w-values for three types of catalysts and two tube diameters [46]. Owing to the high degree of accuracy in the measurement of the temperature profile within the bed and to the computer optimization procedure used to determine the parameters excellent correlations were obtained. The correlations of α_w vs. Reynolds are all linear and show a static contribution in agreement with the theoretical model set up by Yagi & Kunii. The slope was found to depend on the ratio d_t/d_p.

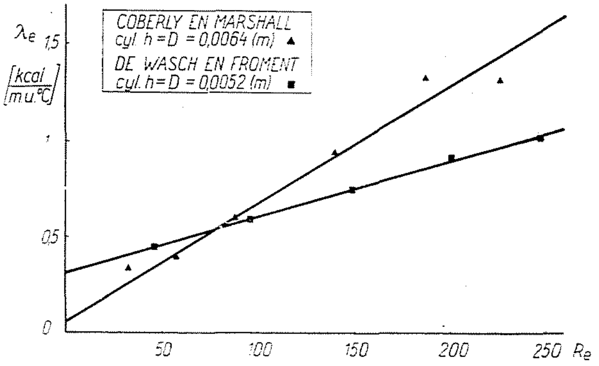

Fig. 18. Comparison of λ_e data of De Wasch & Froment with literature data

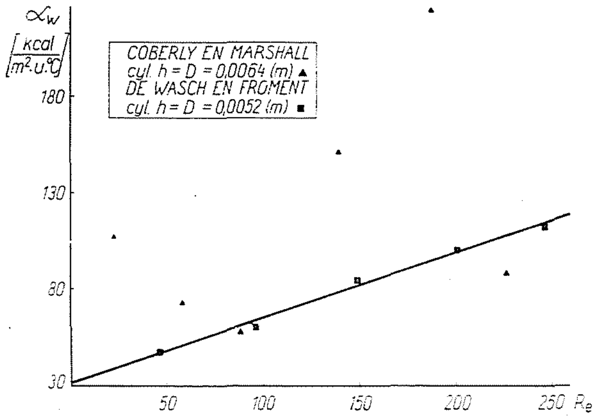

Fig. 19. Comparison of α_w data of De Wasch & Froment with literature data

Figs 18 and 19 compare results obtained by De Wasch & Froment for a phthalic anhydride synthesis catalyst with results of Coberly and Marshall. It is seen how the new data are far more precise.

Heat transfer is not the only phenomenon which is of importance in the design of a chemical reactor, of course. In what preceeds no attention was given to the influence of the rate of reaction. It is evident that the curves of Fig. 10 could be shifted equally well by a slight modification of the kinetic coefficients of the rate equations.

It has to be admitted the accurate prediction of critical situations like those encountered in the case considered requires a degree of precision in the measurement of the experimental parameters which is seldom realized. Yet, even then the approach illustrated in this paper at least permits fixing limits between which the operating conditions in the industrial reactor have to lie. These limits are sufficiently narrow to make the final adjustments of relatively minor importance, so that neither the operating principle nor the expected results are affected by them.

Acknowledgement

The calculations were performed in the Rekenlaboratorium of the Rijksuniversiteit Gent by Dr. W. VANDELEEN and Ir. R. VAN WELSENAERE.

List of symbols

A, B, C	chemical species
A', B', C'	constants in linearized rate equation
a_1	reciprocal of Peclet number for effective radial mass transfer
a_2	reciprocal of Peclet number for effective heat transfer
C	concentration
C_P	specific heat
D_L, D_R	effective diffusivities in axial and radial directions, resp.
D_L', D_R'	effective diffusivities in axial, point values, resp.
d_p	particle diameter
d_t	tube diameter
G	mass flow velocity, superficial
G_t	mass flow velocity, interstitial
ΔH	heat of reaction
k	rate coefficient
M_m	mean molecular weight
N_{A0}, N_0	inlet mole fraction of o-xylene and oxygen, resp.
p	partial pressure of reactant
$r_A, r_B \dots$	rates of reaction
r'	radial co-ordinate
r	reduced radial co-ordinate $= r'/d_p$
R	radius
R'	reduced radius
t	temperature difference between reacting fluid and inlet or coolant temperature
T	absolute temperature
T_0	temperature of feed and coolant, when equal
T_S	coolant temperature
U	overall heat transfer coefficient
u	linear interstitial velocity
w, x, y	conversions
z'	axial co-ordinate
z	reduced axial co-ordinate $= r'/d_p$

α	$\alpha_w d_p/\lambda_R$
α_w^0	wall heat transfer coefficient
α_w	wall heat transfer coefficient under static conditions
λ_L, λ_R	effective thermal conductivities in axial and radial direction, resp.
λ_g	thermal conductivity of the gas
λ_n	set of positive roots of the transcendental equation $\chi \frac{J_1(\chi)}{J_0(\chi)} = \alpha R$ where $J_0(\chi)$ and $J_1(\chi)$ are Bessel functions of the first kind of zero and first order, resp.
$K = \frac{4U}{Gc_p d_t}$	
ψ	a coefficient representative for the lateral mixing near the wall
ϱ_b	catalyst bulk density
Pe_{hR}, Pe_{mL}, Pe_{mR}	Peclet numbers for effective transfer of heat and mass in axial and radial directions
Re	Reynolds number
Pr	Prandtl number
Nu	Nusselt number

Summary

The design of fixed bed catalytic reactors of the tubular type has generally been based upon a so-called one-dimensional model. In this model it is assumed that concentration and temperature gradients only occur in axial direction and that the only transport mechanism operating in this direction is the overall flow itself, considered to be of the plug flow type.

In many cases, however, radial temperature gradients are inevitable in such reactors. The model mentioned above then only leads to average values for the temperatures and conversions and does not provide any information concerning e.g. overtemperatures in the axis, which may be markedly different from the mean and unacceptable for reasons of reactor stability, process selectivity and catalyst deactivation. This paper reports on an investigation of the reliability of the above mentioned model. It is compared with a more elaborate, two-dimensional model that takes the existence of radial gradients into account. The basic data required by this approach are reviewed. The reaction scheme considered is of a relatively complex nature and representative of commercial gas-phase hydrocarbon oxidation.

References

1. Bilous, O.—Amundson, N. R.: A. I. Ch. E. Journal **2**, 117 (1956)
2. Barkelew, C. R.: Chem. Engng. Progr. Symp. Ser. No. 25, Vol. 55—38
3. Van Welsenaere, R.—Froment, G. F.: Chem. Engng. Sci. **25** 1508 (1970)
4. Schwartz—Smith, J. M.: Ind. Engng. Chem. **45**, 1209 (1953)
5. Schertz, W. W.—Bischoff, K. B.: A. I. Ch. E. Journal **15**, 597 (1969)
6. Fahien, R.—Smith, J. M.: A. I. Ch. E. Journal **1**, 25 (1955)
7. Bernard, R. A.—Wilhelm, R.: Chem. Engng. Progr. **46**, 233 (1950)
8. Dorrweiler, V. P.—Fahien, R. W.: A. I. Ch. E. Journal **5**, 139 (1959)
9. Plautz, D. A.—Johnstone, H. F.: A. I. Ch. E. Journal **1**, 193 (1955)
10. Hiby, W.: Symposium "Interaction between fluids and particles" Inst. Chem. Engrs. London 1962
11. McHenry, K. W.—Wilhelm, R. H.: A. I. Ch. E. Journal **3**, 83 (1957)
12. Ebach, E. A.—White, R. R.: A. I. Ch. E. Journal **4**, 161 (1958)
13. Carberry, J. J.—Bretton, R. H.: A. I. Ch. E. Journal **4**, 367 (1958)
14. Strang, D. A.—Geankoplis, C. I.: Ind. Engng. Chem. **50**, 1305 (1958)
15. Cairnes, E. J.—Prausnitz, J. M.: A. I. Ch. E. Journal **6**, 400 (1960)
16. Coberly, C. A.—Marshall, W. R.: Chem. Engng. Progr. **47**, 141 (1951)
17. Campbell, Y. M.—Huntington, R. L.: Petr. Ref. 123 (1952)
18. Calderbank, P. H.—Pogorsky, L. A.: Trans. Instn. Chem. Engrs. **35**, 195 (1957)
19. Kwong, S. S.—Smith, J. M.: Ind. Engng. Chem. **49**, 894 (1957)
20. Kunii, D.—Smith, J. M.: A. I. Ch. E. Journal **6**, 71 (1960)
21. Yagi, S.—Kunii, D.: A. I. Ch. E. Journal **3**, 373 (1957)
22. Singer, E.—Wilhelm, R. H.: Chem. Engng. Progr. **46**, 343 (1950)

23. Hanratty, T. J.: Chem. Engng. Sci. **3**, 209 (1954)
24. Yagi, S.—Wakao, N.: A. I. Ch. E. Journal **5**, 79 (1959)
25. Yagi, S.—Kunii, D.—Wakao, N.: A. I. Ch. E. Journal **6**, 543 (1960)
26. Yagi, S.—Kunii, D.: A. I. Ch. E. Journal **6**, 97 (1960)
27. Leva, M.: Ind. Engng. Chem. **40**, 747 (1948)
28. Verschoor, H.—Schuit, G.: Appl. Sci. Res. **A2**, 97 (1950)
29. Maeda, S.: Techn. Repts. Tohoku Univ. **16**, 1 (1952)
30. Colburn, A. P.: Ind. Engng. Chem. **23**, 190 (1951)
31. Carberry, J. J.—Wendel, M.: A. I. Ch. E. Journal **9**, 129 (1963)
32. Shan-Lin Liu—Amundson, N. R.: Ind. & Engng. Chem. Fund. **1**, 200 (1962); **2**, 183 (1963); Liu, S. L.—Aris, R.—Amundson, N. R.: Ind. Engng. Chem. Fund. **2**, 12 (1963); also: Wicke, E.—Vortmeyer, D.: Z. Elektrochem. **63**, 145 (1959); Wicke, E.: Z. Elektrochem. **65**, 267 (1961)
33. Froment, G. F.: Chem. Engng. Sci. **17**, 849 (1962)
34. Baron, T.: Chem. Engng. Progr. **48**, 118 (1952)
35. Smith, J.: Chemical Engineering Kinetics. McGraw-Hill, London 1956
36. Beek, J.: "Advances in Chemical Engineering" Vol. **3**, 203 (1962)
37. Mickley, H. S.—Letts, R. N.: Can. J. Chem. Eng. **41**, 273 (1963); **42**, 21 (1964)
38. Deans, H. A.—Lapidus, L.: A. I. Ch. E. Journal **6**, 656 (1960)
39. McGuire, M.—Lapidus, L.: A. I. Ch. E. Journal **11**, 85 (1965)
40. Crank, G.—Nicolson, P.: Proc. Camb. Phil. Soc. **43**, 50 (1947)
41. Grosjean, C. C.—Froment, G. F.: Med. Kon. Vl. Acad. België **24**, 1 (1962)
42. Froment, G. F.: Génie Chimique **95**, 41 (1966)
43. Levenspiel, O.—Bischoff, K. B.: "Advances in Chemical Engineering" Vol. **4** (1963)
44. Agnew, J. B.—Potter, D. E.: Trans. Inst. Chem. Engrs. **44**, T. 216 (1966)
45. Froment, G. F.: Ind. Engng. Chem. **59**, 18 (1967)
46. De Wasch, A.—Froment, G. F.: to be published

Prof. Dr. ir. G. Froment, Krijgslaan, 271, Gent, Belgium.